Int. J. Multiphase Flows, Vol. 4, pp. 437–460. Pergamon/Elsevier, 1978. Printed in Great Britain

ON THE DEVELOPMENT OF METHODS FOR ANALYSING TRANSIENT FLOW-BOILING

S. BANERJEE
Professor of Engineering Physics, McMaster University, Hamilton, Ontario, L8S 4M1, Canada

and

W. T. HANCOX
Head, Thermohydraulics Research Branch, Whiteshell Nuclear Research Establishment, Atomic Energy of Canada Limited, Pinawa, Manitoba, ROE 1LO, Canada

(*Received* 20 *February* 1977)

Abstract—A strategy is presented for the development of LOCA analyses. It involves: (i) experiments to determine transfer coefficients needed in the mathematical model and to provide benchmarks to check that the model adequately describes the relevant physical processes, and (ii) development of procedures to determine both benchmark and computationally efficient solutions to the models.

The strategy is illustrated for flow-boiling models of the hyperbolic type. A benchmark solution procedure based on the method of characteristics is outlined. Also outlined are finite difference procedures which require less computation time and are less accurate than the method of characteristics. Both solution procedures, applied to the homogeneous equilibrium model, are shown to adequately predict blowdown benchmark experiments. For the more complex physical situation encountered when cold water is injected into a hot, steam-filled, horizontal channel containing a rod bundle, a thermal non-equilibrium model is shown to provide adequate predictions.

1. PHILOSOPHICAL BASIS

To license water-cooled reactors, postulated loss-of-coolant accidents involving transient two-phase flows must be analyzed. These flows are generally calculated by computer codes such as RODFLOW (Elliott 1968), RELAP (Moore & Rettig 1973) and RELAP-UK (Brittain & Fayers 1976).

The philosophy followed in developing and validating LOCA analysis codes is illustrated in figure 1. The codes are based on a set of field and constitutive equations, and boundary conditions. We will refer to these as the "mathematical model". The field equations express the principles of conservation of mass, momentum and energy. To be of practical use, they contain certain idealizations and averages: for example, the dependent variables may be averaged over the flow cross-section to reduce the field equations to one-dimensional form. The constitutive equations deal with the transfer of mass, momentum and energy across the system boundaries and between phases. They are usually based on correlations of experimental data, although some conclusions regarding their mathematical form can be deduced from more fundamental considerations as suggested by Bouré (1975).

In LOCA analysis codes, the mathematical model is solved by various numerical techniques and the solutions are then compared with experiment to verify the predictive capability of the code. Comparisons with experiment serve to check the idealizations and averages built into the mathematical model (as shown in figure 1). The process of developing a mathematical model usually iterates with experiment, with the insight gained at each stage being used to modify the model to better represent the essential physical processes.

To carry out this process properly, the numerical technique used to solve the model must give the true mathematical solution. Otherwise, the predictions of the code will depend both on the mathematical model and the numerical solution technique. In such a situation comparisons with experiments would be valueless since disagreement (or agreement) could be due to either

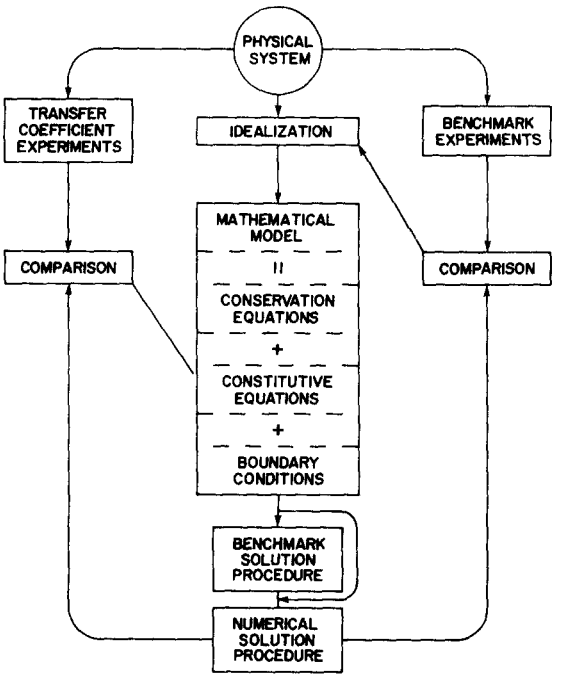

Figure 1. Strategy for model development.

the effect of inaccuracies in the mathematical model or the effect of inaccuracies in the numerical technique or (most likely) both.

In Canada, we have recognised that the practical numerical techniques commonly used in LOCA analysis codes need to be compared against a reference numerical technique. These practical techniques may take much less computer time to solve a problem than the reference technique. However, the reference numerical technique should solve the mathematical problem as exactly as possible so that the solutions can then serve as mathematical standards. Such a reference technique has been developed based on the pure method of characteristics (wave tracing) by Hancox *et al.* (1975). We believe that this method is accurate because its predictions agree with analytical solutions as discussed later. It can be used to calculate accurate solutions only when the mathematical model has real characteristics. This is sufficient, at present, since we have confined our attention to such models.

Development of the reference numerical technique has allowed us to

- isolate the effect of the model(s) on predictions, so that the model(s) can be modified as required by experiment.
- develop computationally faster numerical techniques which calculate solutions with sufficient accuracy compared to the reference technique.

Because of the importance of the reference numerical technique, it is briefly described in section 2 of this paper.

We have also developed two numerical techniques which are computationally faster and more practical for LOCA analysis than the reference technique. Solutions obtained by these techniques appear sufficiently accurate that comparisons of predictions with experiment serve as a check of the mathematical models. They are

- an explicit finite difference technique described and compared with experiments in section 3 (see also Banerjee *et al.* 1975).
- an implicit finite difference technique based on the "characteristic form" of the field equations described in section 4 (see also Mathers *et al.* 1976).

We show in sections 3 and 4 that mathematical models based on the homogeneous equilibrium form of the field equations with simple forms of the constitutive equations are sufficiently accurate in predicting our blowdown experiments.

However, in predicting experiments in which cold water is injected into hot, partially voided systems, more complex field and constitutive equations are found to be necessary to describe the phenomena observed. In section 5, a typical situation in which cold water is injected into a hot horizontal channel is described. The mathematical model based on the physical mechanisms observed is then derived. In doing this, we try to illustrate the role of experiments in guiding the development of the mathematical model—especially the constitutive equations. At the present stage of development, we feel that models more complex than "homogeneous equilibrium" must be based on an understanding of the physical phenomena that occur in a particular portion of the flow circuit during various stages of the flow transient. A knowledge of flow regimes is particularly important in deriving the constitutive equations and minimizing the number of free parameters.

The paper is concluded with a summary of plans for future developments.

2. THE REFERENCE NUMERICAL TECHNIQUE

The reference numerical technique is based on the method of characteristics (wave tracing). The mathematical models that may be solved by the technique have the form

$$\frac{\partial \bar{U}}{\partial t} + \tilde{A}(\bar{U})\frac{\partial \bar{U}}{\partial z} = \bar{C}(\bar{U}) \qquad [1]$$

where $\bar{U}$, vector of dependent variables: $\tilde{A}$, matrix of coefficients which are functions of U; $\bar{C}$, vector describing heat, mass and momentum transfer between system boundaries and flow, and between vapour and liquid phases.

Equation [1] must be hyperbolic to be solved by the method of characteristics; this is so when the eigenvalues of $\tilde{A}$ are real. To illustrate the use of the method of characteristics, the simplest one-dimensional flow model, homogeneous equilibrium flow has been chosen.

For homogeneous equilibrium flow,

$$\bar{U} = \begin{bmatrix} u \\ H \\ P \end{bmatrix}, \qquad \bar{C} = \begin{bmatrix} -F - g\dfrac{\mathrm{d}Z}{\mathrm{d}z} \\ a^2(Q+uF)\left.\dfrac{\partial \rho}{\partial P}\right|_H - \dfrac{u}{A}\dfrac{\mathrm{d}A}{\mathrm{d}z} \\ a^2\left[-\dfrac{\rho u}{A}\dfrac{\mathrm{d}A}{\mathrm{d}z} - (Q+uF)\left.\dfrac{\partial \rho}{\partial H}\right|_P\right] \end{bmatrix} \equiv \begin{bmatrix} C_1 \\ C_2 \\ C_3 \end{bmatrix},$$

$$\tilde{A} = \begin{bmatrix} u & 0 & 1/\rho \\ a^2 & u & 0 \\ \rho a^2 & 0 & u \end{bmatrix} \quad \text{where } a = \left[\frac{1}{\rho}\left.\frac{\partial \rho}{\partial H}\right|_P + \left.\frac{\partial \rho}{\partial P}\right|_H\right]^{-1/2}. \qquad [2]$$

The eigenvalues of $\tilde{A}$, called characteristic directions, are:

$$\frac{\mathrm{d}z}{\mathrm{d}t} = u, \quad u+a, \quad u-a. \qquad [3]$$

The ordinary differential equations, called compatibility equations, along the characteristic directions are:

$$\text{along } \frac{\mathrm{d}z}{\mathrm{d}t} = u + a$$

$$\mathrm{d}P + \rho a\,\mathrm{d}u = (C_3 + \rho a C_1) \equiv K\mathrm{d}t, \qquad [4]$$

$$\text{along}\frac{dz}{dt} = u - a$$

$$dP - \rho a\,du = (C_3 - \rho a C_1) \equiv L\,dt, \qquad [5]$$

$$\text{along}\frac{dz}{dt} = u$$

$$dP - \rho\,dH = (C_3 - \rho C_2) \equiv M\,dt. \qquad [6]$$

Here u is the velocity, a, the equilibrium sound speed, H, ρ, the mixture enthalpy and density, Z, the elevation, z, space coordinate, F, friction force per unit mass, g, acceleration of gravity, P, the pressure, A, the cross section area and Q is the heat added per unit mass. To solve [1] and [2], values of (u, P, H) are calculated from finite difference approximations to the compatibility equations [4] to [6] using the code MECA (Hancox *et al.*, 1975; Hancox & Banerjee 1977).

To illustrate the type of results obtained, we show in figure 2 the characteristics $u \pm a$ for the early stages in the blowdown of a 4 m pipe of 32 mm I.D. filled with subcooled water at 7.0 MPa and 243°C (Edwards & O'Brien 1970). The sharp change in the characteristics shows the boiling boundary and is due to the sharp reduction in the speed of sound in the two-phase region. The dependent variables (u, P, H) are of course known at each intersection.

The particle paths $((dz/dt) = u)$ are shown in figure 3 for the whole blowdown. The particles can be seen to accelerate as the expansion waves progress from right to left. At the end of blowdown, the flow reverses at the open end because the internal pressure due to outflow inertia is less than the receiver pressure for a brief period. The other variables calculated will be shown in the next section where comparisons are made between various numerical techniques and experimental results.

The same technique has been used for more complex equations of the form [1] (Ferch 1978). If $u = u_G = u_L$, and the vector $\bar{C}(\bar{U})$ does not contain derivatives of $\bar{U}$, then the characteristics are:

$$\frac{dz}{dt} = u, u, u, u + a', u - a',$$

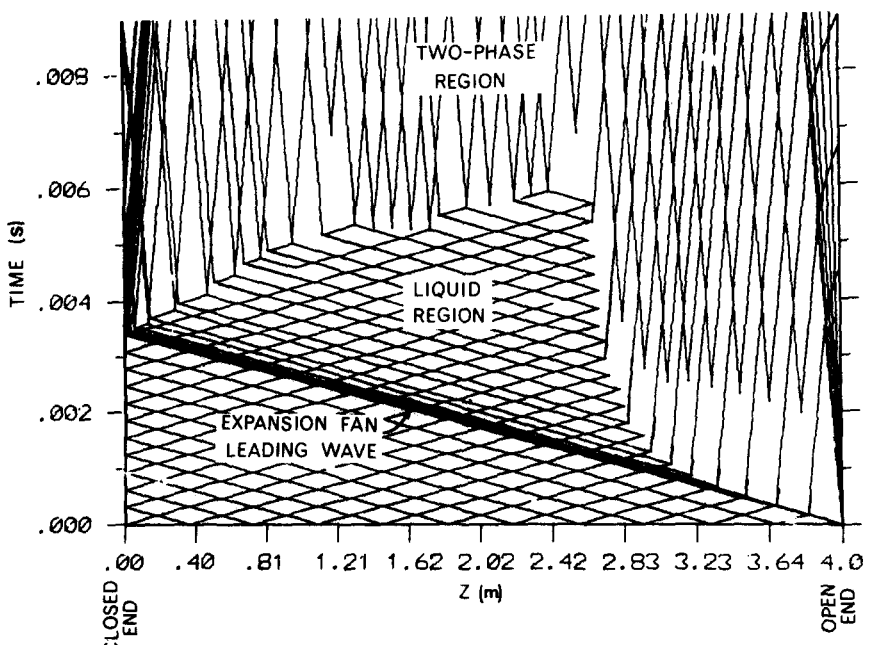

Figure 2. Initial development of the $dz/dt = u \pm a$ characteristics.

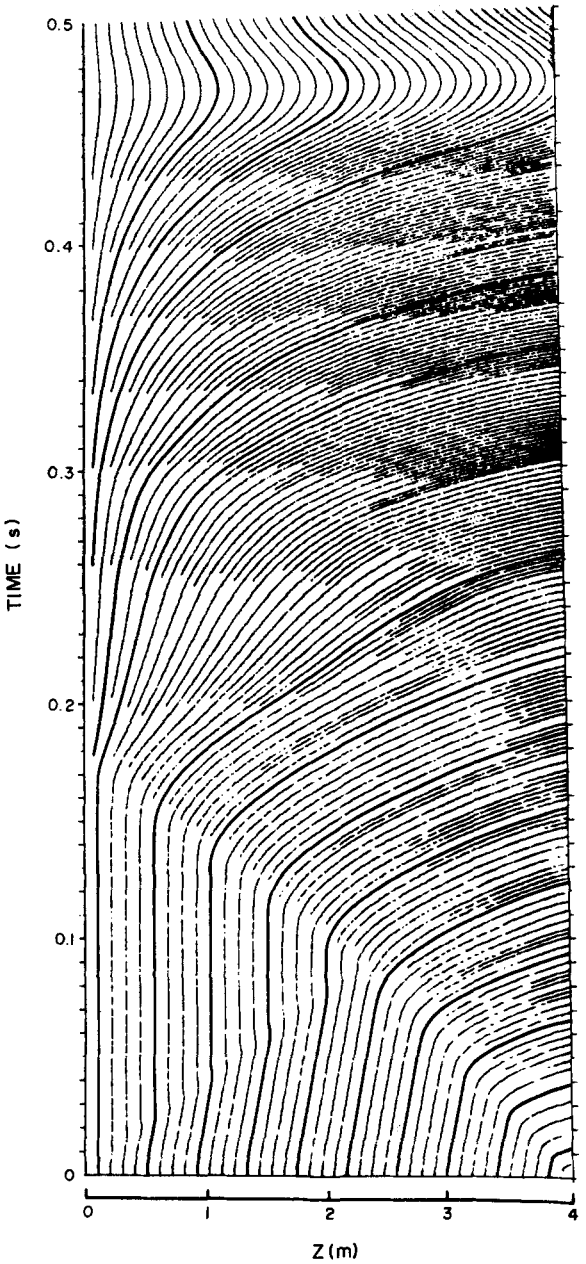

Figure 3. $(dz/dt) = u$ characteristics; path of individual fluid particles.

where

$$a' = \text{sound speed} = \left[\rho\left\{\frac{1-\alpha}{\rho_L a_L^2} + \frac{\alpha}{\rho_G a_G^2}\right\}\right]^{-1/2} \quad [7]$$

The compatibility equations are:

$$\text{along}\,\frac{dz}{dt} = u + a'$$

$$dP + \rho a' du = \left\{\frac{\rho a'^2(\rho_G C_5 + \rho_L C_4)}{\rho_L \rho_G} + a' C_1\right\} dt, \quad [8]$$

$$\text{along}\,\frac{dz}{dt} = u - a'$$

$$dP - \rho a' du = \left\{\frac{\rho a'^2(\rho_G C_5 + \rho_L C_4)}{\rho_L \rho_G} - a' C_1\right\} dt \quad [9]$$

$$\text{along}\ \frac{dz}{dt} = u$$

$$d\alpha - \frac{\alpha(1-\alpha)(\rho_G a_G^2 - \rho_L a_L^2)}{\rho_G a_G^2 \rho_L a_L^2} dP = \frac{(1-\alpha)\rho_L C_4 - \alpha\rho_G C_5}{\rho_L \rho_G} dt, \quad [10]$$

$$(1-\alpha)\rho_L dh_L - (1-\alpha)\, dP = C_7 dt, \quad [11]$$

$$\alpha\rho_G dh_G - \alpha dP = C_6 dT. \quad [12]$$

where α is the void fraction. The dependent variables are u, P, α, h_L and h_G. The vector $\bar{C}$ is defined later in [31] to [35]. The solution is also advanced by a wave tracing procedure (Ferch 1978).

3. EXPLICIT FINITE DIFFERENCE TECHNIQUE

Description of technique

A code (RODFLOW) has been developed (Banerjee *et al.* 1975) based on the one-dimensioal conservation equations assuming thermal equilibrium between vapour and liquid. An explicit finite difference technique is used to solve the following equations which are written in the form of the "conservation law":

$$A\frac{\partial \rho}{\partial t} + \frac{\partial}{\partial z}(AG) = 0, \quad [12']$$

$$A\frac{\partial E}{\partial t} + \frac{\partial}{\partial z} AG\left[H + \frac{G^2 v''}{2\rho^2}\right] = Aq''', \quad [13]$$

$$A\frac{\partial G}{\partial t} + \frac{\partial}{\partial z}\left[A\frac{G^2}{\rho}v'\right] + A\frac{\partial P}{\partial z} + A\rho g\frac{dZ}{dz} + A\tau = 0, \quad [14]$$

where

$$E = \rho\left(e + \frac{G^2 v'}{2\rho^2}\right),$$

$$H = Xh_G + (1-X)h_L$$

$$v' = \frac{X^2}{x} + \frac{(1-X)^2}{1-x}; \qquad v'' = \frac{X^3}{x^2} + \frac{(1-X)^3}{(1-x)^2},$$

$$e = xe_G + (1-x)e_L.$$

where G is the mass velocity; h_k and e_k is phase k enthalpy and internal energy, respectively and τ is the frictional force.

In the above equations, x and X are the thermodynamic and flow qualities, respectively. In RODFLOW, they must be related by an empirical "slip" relationship. For the cases discussed here, no relative velocity is assumed, i.e. $x = X$.

The system of equations is closed with the following constitutive equations:

(i) equation of state $P = P(e,\rho)$.

(ii) τ = frictional force per unit volume.

(iii) q''' = heat added at the boundaries per unit volume.

(iv) correlation for relative velocity if any.

To solve these equations, the system is divided into control volumes with fluid properties defined at the centroid and mass velocities at the boundaries. For the general element shown in figure 4, the conservation equations are approximated by

$$\left(\frac{d\rho}{dt}\right)_j = \frac{(AG)_{j-1/2} - (AG)_{j+1/2}}{A_j \Delta z_j} \quad [15]$$

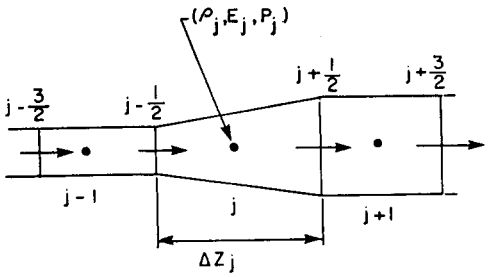

Figure 4. Schematic of finite difference element (RODFLOW).

For $G_{j+1/2} > 0$,

$$\left(\frac{dE}{dt}\right)_j = \frac{1}{A_j \Delta z_j}\left[(AG)_{j-1/2}\left\{H_{j-1} + \frac{G^2_{j-1/2}\,\nu''_{j-1}}{2\rho_{j-1}}\right\} - (AG)_{j+1/2}\left\{H_j + \frac{G^2_{j+1/2}\,\nu''_j}{2\rho_j}\right\}\right] + q'''_j \quad [16]$$

$$\left(\frac{dG}{dt}\right)_{j+1/2} = \frac{1}{A_{j+1/2}\Delta z_j}\left[\frac{(AG^2)_{j-1/2}\nu'_{j-1}}{\rho_{j-1}} - \frac{(AG^2)_{j+1/2}\nu'_j}{\rho_j}\right] - \frac{P_j - P_{j+1} - \rho_j g \Delta Z_{j+1/2}}{(\Delta z_j + \Delta z_{j+1})/2} - \tau_{j+1/2} \quad [17]$$

For $G_{j+1/2} < 0$,

$$\left(\frac{dE}{dt}\right)_j = \frac{1}{A_j \Delta z_j}\left[(AG)_{j+1/2}\left\{H_{j-1} + \frac{G^2_{j-1/2}\nu''_j}{2\rho_j}\right\} - (AG)_{j+1/2}\left\{H_{j+1} + \frac{G^2_{j+1/2}\nu''_{j+1}}{2\rho_{j+1}}\right\}\right] + q'''_j \quad [18]$$

$$\left(\frac{dG}{dt}\right)_{j+1/2} = \frac{1}{A_{j+1/2}\Delta z_{j+1}}\left[\frac{(AG^2)_{j+1/2}\nu'_{j+1}}{\rho_{j+1}} - \frac{(AG^2)_{j+3/2}\nu'_{j+2}}{\rho_{j+2}}\right] - \frac{P_j - P_{j+1} - \rho_j g \Delta Z_{j+1/2}}{(\Delta z_j + \Delta z_{j+1})/2} - \tau_{j+1/2} \quad [19]$$

This precedure results in a system of $3N$ ordinary differential equations which may be solved by a variety of integration techniques. We have used the simplest integration technique by approximating the time derivatives by

$$\left(\frac{df}{dt}\right)_c = \frac{f_c^{n+1} - f_c^n}{\Delta t}, \quad [20]$$

where superscript n denotes the value at the nth time step.

The maximum time step that can be used with the above integration procedure is determined by

$$\left(\frac{G}{\rho} + a\right)\frac{\Delta t}{\Delta z} < 1, \quad [21]$$

where a is the speed of sound for homogeneous equilibrium flow

$$a = \left[\left|\frac{\partial \rho}{\partial P}\right|_H + \frac{1}{\rho}\left|\frac{\partial \rho}{\partial H}\right|_P\right]^{-1/2}$$

The boundary condition used at the break is

$$P_{exit} = \text{receiver pressure if } u_{exit} < a_{exit},$$

otherwise

$$u_{exit} = a_{exit}.$$

Comparison with reference numerical technique and experiment

Some results of comparisons between experiment, the reference numerical technique and the explicit finite difference technique are discussed in this section to illustrate the main features. The conservation equations solved were for homogeneous, equilibrium two-phase flow.

The first comparison is based on the experiments reported by Edwards & O'Brien (1970). A closed cylindrical pipe (4 m long and of 32 mm I.D.) at 7.0 MPa and 243°C was suddenly opened at one end to atmospheric pressure. The resulting pressure and density transient was measured at several locations. The pressure transient at the closed end is shown in figure 5 and compared with calculations based on the homogeneous equilibrium model. Calculations by the method of characteristics (MECA) and the explicit finite difference technique (RODFLOW) are also shown in the figure. As mentioned earlier the method of characteristics can be compared directly with analytical solutions for the propagation of the initial expansion wave. The pressure transient predicted by MECA, shown in the upper curve on figure 5, is in exact agreement with the corresponding analytical solution. Whereas, the finite difference solutions clearly show numerical diffusion. The characteristic finite difference technique (RAMA) will be discussed later. Two effects are apparent

- the explicit finite difference technique (RODFLOW) tends to diffuse the very sharp changes in pressure that are predicted by MECA (and seen experimentally) when the first rarefaction wave reaches the closed end at about 3 ms;
- the experimentally measured pressures generally lie below the saturation pressure (for the initial conditions reported by Edwards & O'Brien 1970) and there is a sharp pressure undershoot between 3 and 5 ms.

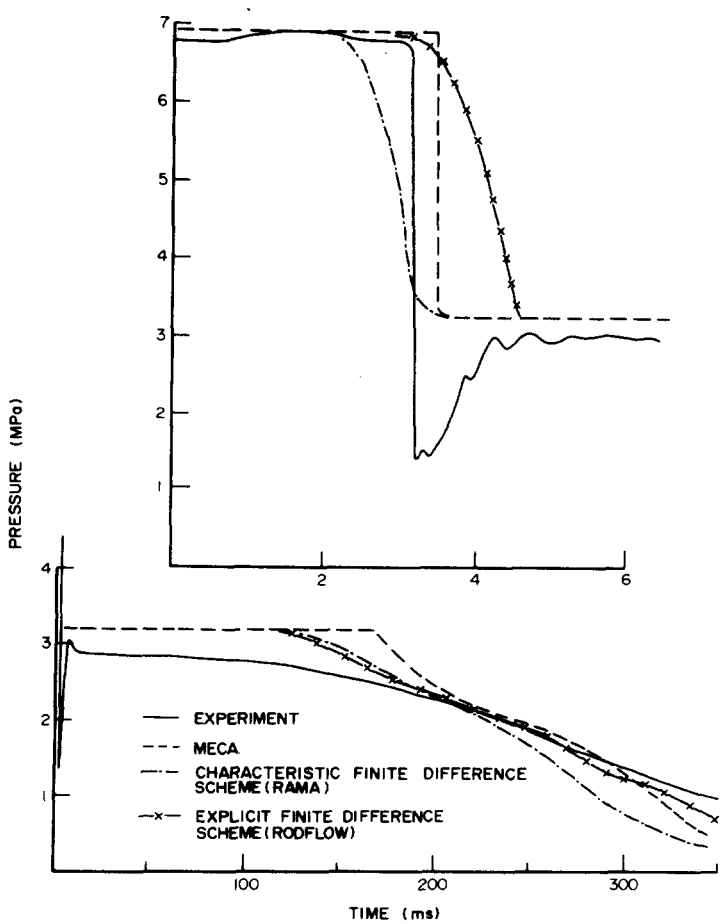

Figure 5. Comparison of predicted and experimental values of pressure at the closed end.

The first effect is typical of finite difference schemes in that discontinuities calculated by the method of characteristics tend to be rounded off due to numerical diffusion. This difference does not affect predictions of sheath temperature and other important features of the transient as shown later.

The second effect, we ascribe to a delay in bubble (or void) formation and growth. Such effects can only be calculated by mathematical models which allow thermal non-equilibrium between phases. The homogeneous equilibrium model cannot predict these non-equilibrium effects, but does predict the main features of the transient.

The second comparison is based on the experiments reported by Banerjee *et al.* (1975) and in more detail by Premoli & Hancox (1976). In this experiment, flow was established through the test section shown in figure 6. Quick acting valves 2 and 5 were closed and valve 1 opened simultaneously. The fluid trapped between valves 2 and 5 discharged from the test section and pressure, temperature and mass holdup in various parts of the test section were measured. A wide range of initial conditions and break areas was investigated about a set of reference conditions. These experiments differ from those reported by Edwards & O'Brien (1970) in that heat was added during the blowdown and the fluid was flowing when the rupture was initiated.

Figure 7 shows the pressure transients calculated and measured for the reference experiment. The method of characteristics calculation (MECA) again shows sharper changes than calculated by the explicit finite difference technique (RODFLOW), otherwise the calculations are in reasonable agreement with each other. RODFLOW calculations are compared with the mass held up in the heated section for several different initial conditions in figure 8; the agreement is quite good. Sheath temperatures predicted by RODFLOW and measured in the experiment are shown for two different cases in figure 9. Again the agreement is good though RODFLOW predicts the onset of CHF somewhat earlier than observed experimentally for the 120°C inlet subcooling case. The sheath temperatures predicted are relatively insensitive to the correlations for onset of CHF and post dryout heat transfer. This is because the onset of CHF is primarily caused by a lack of water at that location. This is supported by measurements of mass holdup in the heated section reported by Premoli & Hancox (1976). The heated section average void fraction at CHF was greater than 98% in all cases. Therefore, agreement cannot

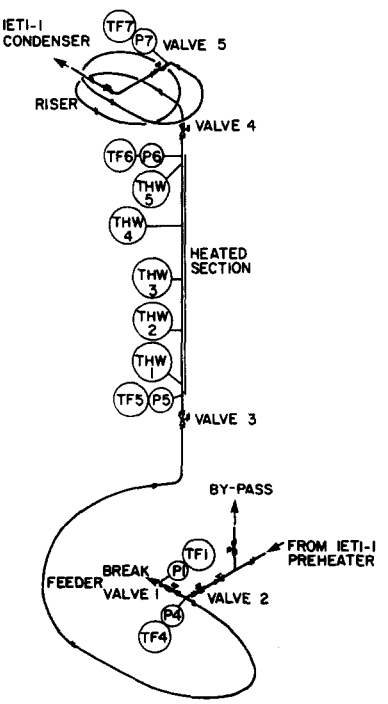

Figure 6. IETI-1 test section schematic drawing.

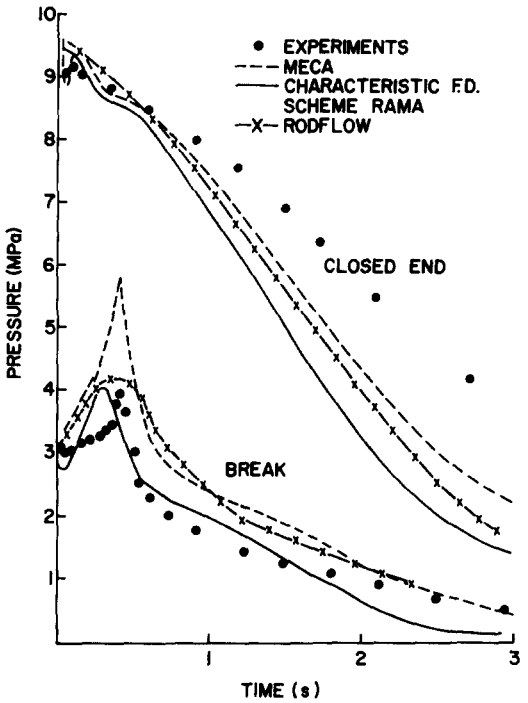

Figure 7. Comparison of predictions with IETI-1 experimental data: pressure history.

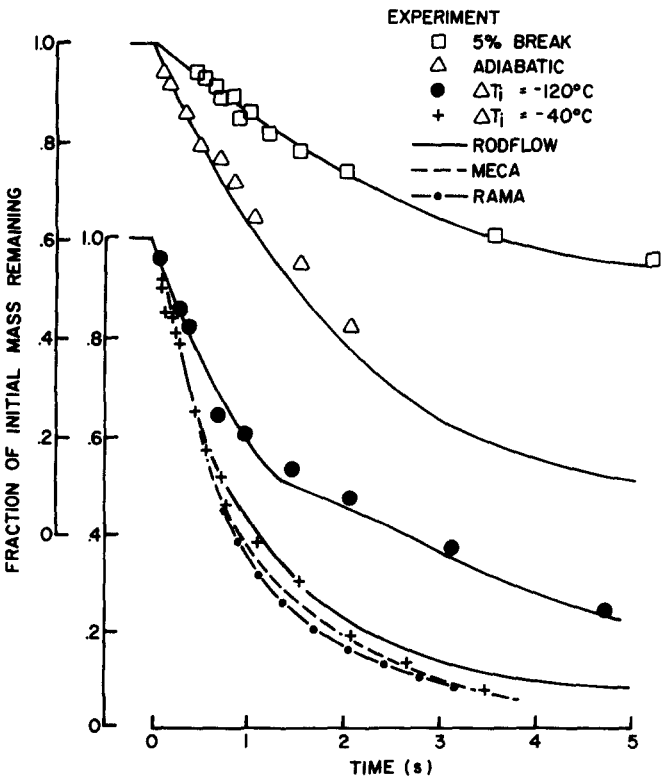

Figure 8. Time variation of mass holdup.

be obtained by simply changing the correlation for onset of CHF. For the 120°C subcooling case, we feel that non-equilibrium effects are important and have to be accounted for to reduce conservatism in the RODFLOW predictions.

A series of more complicated blow down experiments was done in the loop shown in figure 10 to test the predictive capability of computer codes (Arrison *et al.* 1977). The mathematical

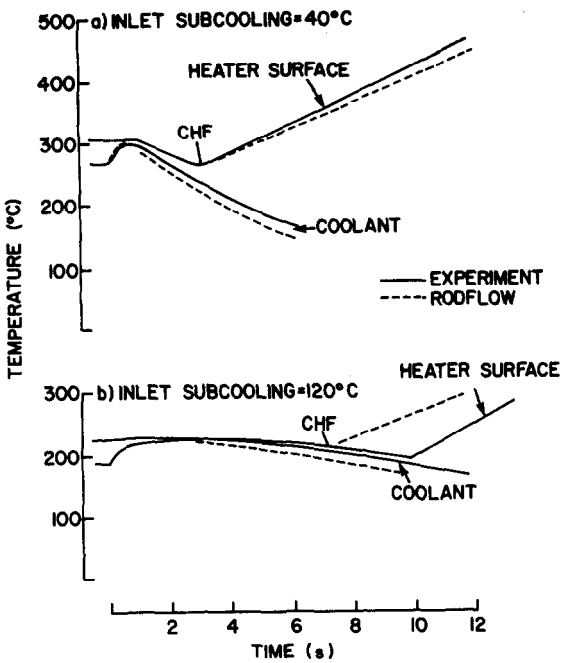

Figure 9. Heater surface and coolant temperatures at the heated section inlet.

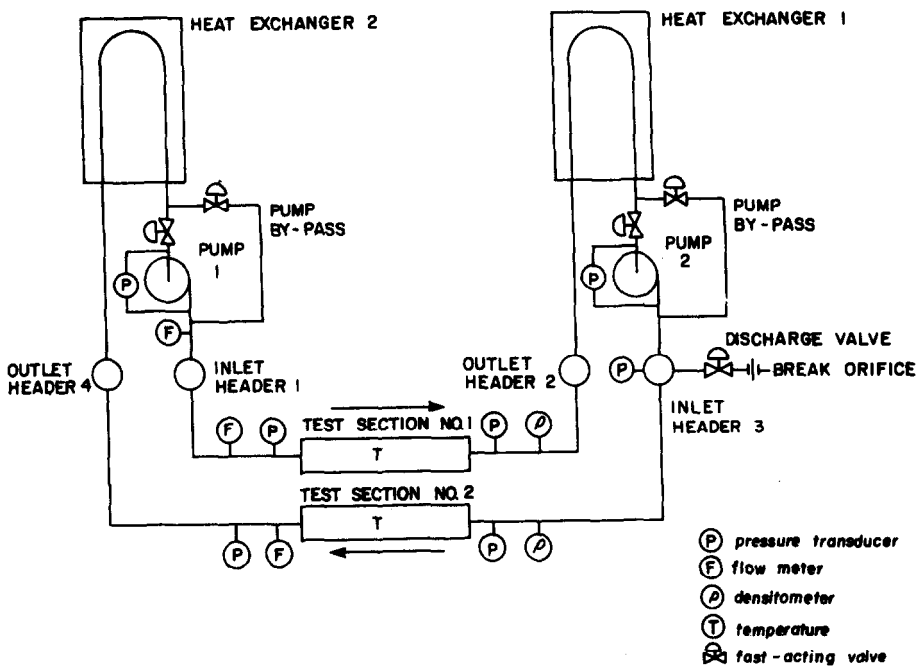

Figure 10. RD-4 loop schematic.

model was exactly the same as for the comparisons discussed above. The only additional equation was for pump behaviour in steam–water flow. The pump model was taken to be the same as proposed by the Aerojet Nuclear Company (1974) for the Semiscale pump even though measurements showed that our pump behaved somewhat differently. The calculations were all done with the explicit finite difference code RODFLOW since the method of characteristics required too much computer time.

The experimental facility consisted of pumps, heaters, and heat exchangers arranged in a "figure of eight" circuit typical of Canadian reactors and containing all the essential features. Pressures, temperatures, coolant densities and flow rates were measured at many points in the

circuit for inlet header breaks of various sizes. Experiments were done both with the pumps operating in the loop during the blowdown and with the pumps bypassed. The circuit was usually brought to a steady initial state and blowdown was started by opening a quick-acting valve connected to inlet header 1. In most of the experiments the power was held at the initial conditions for the first 7 sec of blowdown and then abruptly reduced to 10% of the initial level and maintained at the reduced level to the end of blowdown. The experimental facility and measurements will be described fully in a subsequent paper. Here, only some typical heater surface temperature comparisons are shown to illustrate the main points.

Heater temperatures measured for a 50% inlet header break with the pumps bypassed are shown in figure 11 and compared with RODFLOW. Note that RODFLOW was not "tuned" to fit the experiment so the initial temperature predicted is somewhat high. Also, the onset of CHF is predicted to occur somewhat earlier than experimentally observed for test section 1. The shape of the temperature transient is predicted well. We also note that flow rates, pressures and coolant densities at other loop locations were predicted accurately.

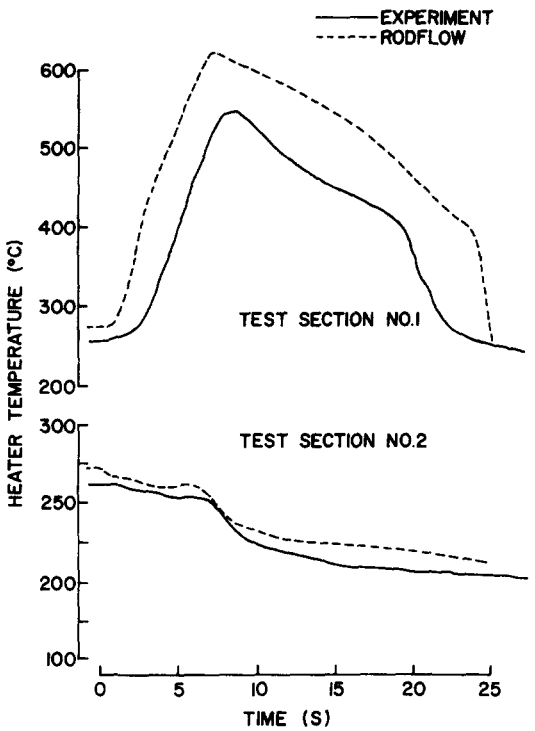

Figure 11. Heater temperature history; 50% break with pumps by-passed.

Figure 12 summarizes the results of a large number of experiments with the pumps operating throughout the blowdown. The maximum temperature reached is shown for various break sizes. For the facility geometry and initial conditions investigated in these experiments, the highest temperatures occurred for breaks between 10 and 15% of the pipe cross-sectional area. RODFLOW predictions are also shown on the figure and are somewhat higher. This conservatism is again due to the onset of CHF being predicted earlier in the blowdown than actually observed. Changing the correlation for onset of CHF does not affect the results. Our experiments show a very small pressure difference across the heated section at onset of CHF, indicating a low mass velocity. A heat balance based on a homogeneous equilibrium model, shows that there would be a very sharp decrease in density. This leads to a somewhat earlier onset of CHF than would a thermal non-equilibrium model. Thus to reduce conservatism in the predictions, in our opinion, the field equations must take non-equilibrium into account; adjusting the constitutive equations will not have this effect since the results are relatively insensitive to them.

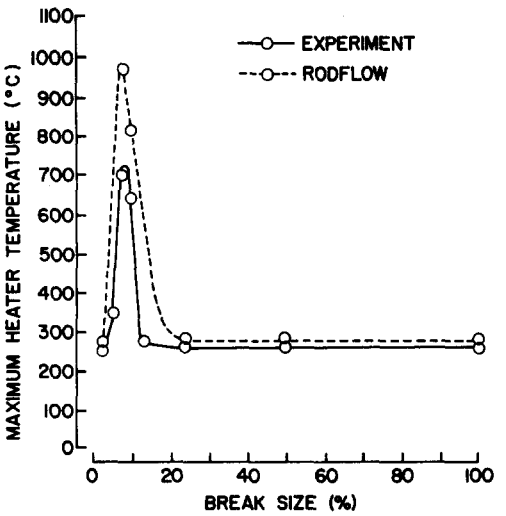

Figure 12. Maximum heater temperature vs break size.

Also, the predictions of the sheath temperature transients were not very sensitive to the model used for pump behaviour. Inserting the measured pressure difference across the pumps into the code in place of the ANC pump model did not markedly change the predictions. This result is of course specific to this particular facility and set of experiments.

The main conclusions are:

- the explicit finite difference technique described solves the mathematical model accurately; this conclusion is based on comparisons with our reference technique—the method of characteristics,
- mathematical models based on homogeneous equilibrium flow are adequate for modelling the blowdown experiments we have investigated but,
- the sheath temperatures predicted by the homogeneous equilibrium model are higher than in experiments and we feel this conservatism can be reduced by a mathematical model which allows thermal non-equilibrium between phases.

4. THE CHARACTERISTIC FINITE DIFFERENCE TECHNIQUE

The explicit finite difference technique is much faster than the reference numerical technique and can therefore be used to calculate LOCA transients of practical interest.

However, it has the following disadvantages:

- very large amounts of computer time are still required because of the limitation on time step for numerical stability,
- extensions to solve more complex mathematical models, which take thermal non-equilibrium between phases into account are not easy,
- it does not handle boundary conditions naturally (as does the method of characteristics), so calculations for pipe networks with many branches are difficult.

A finite difference technique has been developed to solve these problems and is now described.

Description of technique

The equations for one dimensionsal transient two-phase flow are represented by [1]. If the matrix $\tilde{A}$ has real eigenvalues, then the equation can be written as:

$$\tilde{B}\frac{\partial \bar{U}}{\partial t}+\tilde{\Lambda}\tilde{B}\frac{\partial \bar{U}}{\partial z}=\bar{D}, \qquad [22]$$

where the columns of $\tilde{B}^{-1}$ are the eigenvectors of $\tilde{A}$, $\tilde{\Lambda}$ is a diagonal matrix of eigenvalues of $\tilde{A}$ and $\tilde{D} = \tilde{B}\tilde{C}$. For homogeneous equilibrum flow,

$$\tilde{U} = \begin{bmatrix} u \\ H \\ P \end{bmatrix}; \quad \tilde{B} = \begin{bmatrix} \rho a & 0 & 1 \\ 0 & 1 & -1/\rho \\ -\rho a & 0 & 1 \end{bmatrix}; \quad \tilde{\Lambda} = \begin{bmatrix} u+a & & \\ & u & \\ & & u-a \end{bmatrix}$$

and

$$\tilde{D} = \begin{bmatrix} C_3 + \rho a C_1 \\ -(C_3/\rho) + C_2 \\ C_3 - \rho a C_1 \end{bmatrix}, \qquad [23]$$

where $\rho = \rho(H,P)$ and $\tilde{C}$ has been defined previously.

Comparison of this form with that for the method of characteristics shows that the first and last equations are equivalent to the compatibility equations [4] and [5] along the $(u+a)$ and $(u-a)$ characteristics, and the middle equation is equivalent to the compatibility equation [6] along the particle path, u. Hence this form is callled the characteristic form of the field equations.

Consider the space–time mesh in figure 13. The following left and right hand difference approximations may be written for [22] about the kth mesh line:

$$\tilde{B}_k^n \frac{\tilde{U}_k^{n+1} - \tilde{U}_k^n}{\Delta t} + \tilde{\Lambda}_k^n \tilde{B}_k^n \frac{\tilde{U}_k^{n+1} - \tilde{U}_{k-1}^{n+1}}{\Delta z_{k-1}} = \tilde{D}_k^n, \qquad [24]$$

$$\tilde{B}_k^n \frac{\tilde{U}_k^{n+1} - \tilde{U}_k^n}{\Delta t} + \tilde{\Lambda}_k^n \tilde{B}_k^n \frac{\tilde{U}_{k+1}^{n+1} - \tilde{U}_k^{n+1}}{\Delta z_k} = \tilde{D}_k^n. \qquad [25]$$

Whether the difference form [24] or [25] is used depends on the flow character at mesh k as shown in figure 14. Here the spatial derivatives are always approximated by left hand differences when the characteristic is positive and right hand differences when the characteristic is negative, e.g. for supersonic flow to the right all three equations use spatial difference operators which point upstream of k. These conventions make the finite difference equations as similar as possible to the method of characteristics.

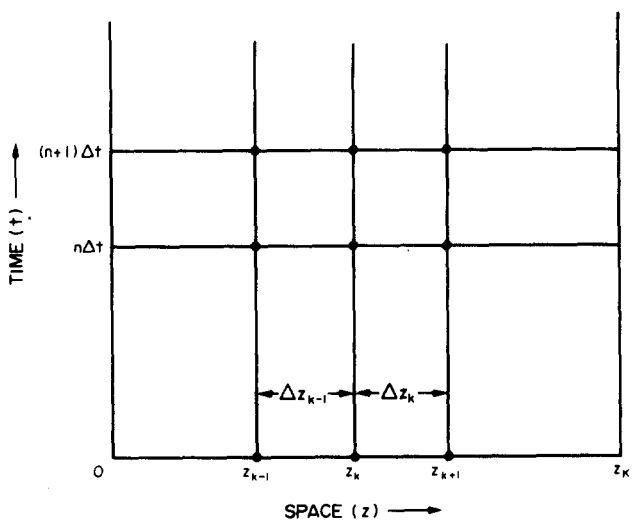

Figure 13. Solution grid in the space–time plane.

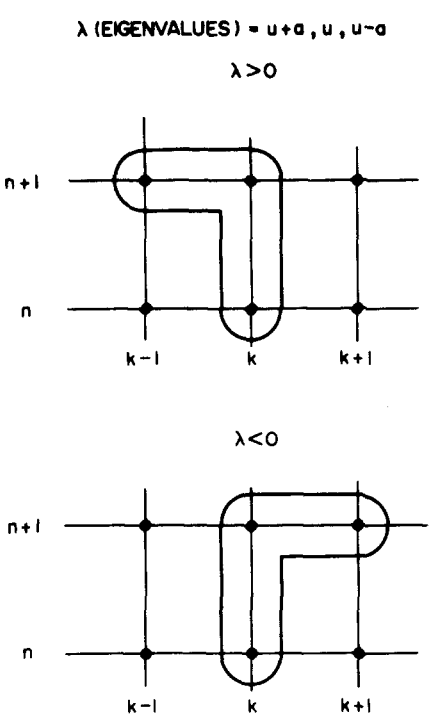

Figure 14. Characteristic finite difference computation molecules.

Combining [24] and [25] we have the kth difference equation:

$$\tilde{M}_{k,k-1}\bar{U}_{k-1}^{n+1} + M_{k,k}\bar{U}_k^{n+1} + \tilde{M}_{k,k+1}\bar{U}_{k+1}^{n+1} = N_k, \qquad [26]$$

where $k = 2,3,\ldots,k-1$.

The components of the 3×3 matrices $\tilde{M}_{k,k-1}$,$\tilde{M}_{k,k}$ and $\tilde{M}_{k,k+1}$ are:

$$\tilde{M}_{k,k-1} = \tilde{\Gamma}[-\tilde{\Omega}\tilde{\Lambda}_k\tilde{B}_k + (\tilde{I}-\tilde{\Omega})(\lambda_{k-1}\tilde{I} - \tilde{\Lambda}_{k-1})\tilde{B}_{k-1}], \qquad [27]$$

$$\tilde{M}_{k,k} = \tilde{\Omega}[(\tilde{I}-\tilde{\Gamma})\lambda_k + \tilde{\Gamma}\lambda_{k-1} - (\tilde{I}-2\tilde{\Gamma})\tilde{\Lambda}_k]\tilde{B}_k + (\tilde{I}-\tilde{\Omega})[\tilde{\Gamma}\tilde{\Lambda}_{k-1}\tilde{B}_{k-1} - (\tilde{I}-\tilde{\Gamma})\tilde{\Lambda}_{k+1}\tilde{B}_{k+1}], \qquad [28]$$

$$\tilde{M}_{k,k+1} = (\tilde{I}-\tilde{\Gamma})[\tilde{\Omega}\tilde{\Lambda}_k\tilde{B}_k + (\tilde{I}-\tilde{\Omega})(\lambda_k\tilde{I} + \tilde{\Lambda}_{k+1})\tilde{B}_{k+1}] \qquad [29]$$

and the column vector $\bar{N}_k$:

$$\bar{N}_k = \tilde{\Omega}[(\tilde{I}-\tilde{\Gamma})\Delta z_k + \tilde{\Gamma}\Delta z_{k-1})D_k + (\tilde{I}-\tilde{\Gamma})\lambda_k + \tilde{\Gamma}\lambda_{k-1})\tilde{B}_k\bar{U}_k^n] + (\tilde{I}-\tilde{\Omega})[\tilde{\Gamma}\tilde{D}_{k-1}\Delta z_{k-1} + (\tilde{I}-\tilde{\Gamma})\tilde{D}_{k+1}\Delta z_k + \lambda_{k-1}\tilde{\Gamma}\tilde{B}_{k-1}\bar{U}_{k-1}^n + \lambda_k(\tilde{I}-\tilde{\Gamma})\tilde{B}_{k+1}\bar{U}_{k+1}^n], \qquad [30]$$

where $\lambda_k = \Delta z_k/\Delta t$.

The essence of the method lies in the choice of $\tilde{\Gamma}$. For homogeneous equilibrium flow, if we have at mesh k,

(i) Supersonic flow from left to right, then

$$\tilde{\Gamma} = \tilde{I};$$

(ii) Subsonic flow from left to right, then

$$\tilde{\Gamma} = \begin{bmatrix} 1 & & \\ & 1 & \\ & & 0 \end{bmatrix};$$

(iii) Subsonic flow from right to left, then

$$\tilde{\Gamma} = \begin{bmatrix} 1 & & \\ & 0 & \\ & & 0 \end{bmatrix};$$

(iv) Supersonic flow from right to left, then

$$\tilde{\Gamma} = 0.$$

Usually $\tilde{\Omega} = \tilde{I}$, but in some special situations where property derivatives are changing rapidly (in low quality regions) it may be used as a weighting matrix.

If mesh points 1 and K are the boundaries of a branch then [26] is applied to these points as well. Any difference equations which have subscripts of either 0 or $K+1$ are dropped from the set and appropriate boundary conditions supplied in their place. This ensures that the boundary conditions used are necessary and sufficient for the original problem. Junctions, discontinuities (such as area changes, pressure rise at a pump, etc.), and unequal segment lengths are easily handled.

For a pipe branch divided into $K-1$ segments, [26] with boundary conditions, results in a set of $3K$ linear algebraic equations with $3K$ unknowns. The equations have the banded matrix structure shown in figure 15. The structure of the band matrices showing their flow direction dependence is shown in figure 16 for subsonic flow. These equations can be solved efficiently, because of the banded matrix structure, by using a special algorithm based on the Gauss elimination method, which takes advantage of zero elements.

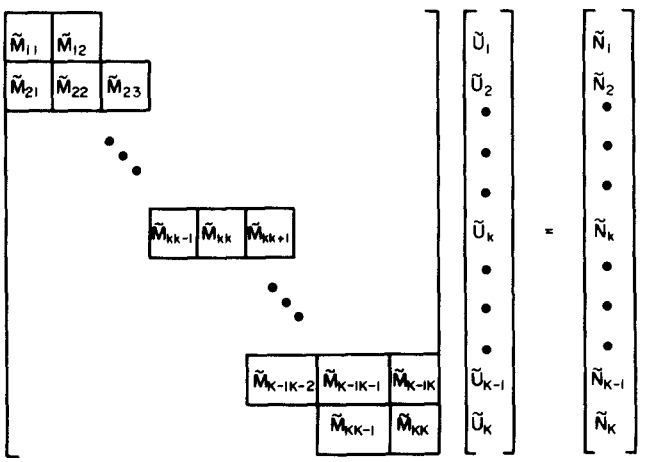

Figure 15. Structure of the system of $3K$ linear algebraic equations.

For certain choices of dependent variables such as $\tilde{U}^T = [u, H, P]$, the boiling boundary requires special treatment to conserve mass exactly as discussed by Mathers *et al.* (1976). For some problems the choice $\tilde{U}^T = [G, H, P]$ may simplify the treatment required.

The numerical technique described in this section has been programmed into a computer code RAMA. RAMA solves one-dimensional flow problems described by [1] when the characteristics are real. In the next section, an application to flows with unequal phase temperatures (thermal non-equilibrium between phases) is described. In this section we will discuss comparisons with blowdown experiments and the reference numerical technique (MECA) using the homogeneous equilibrium model [2].

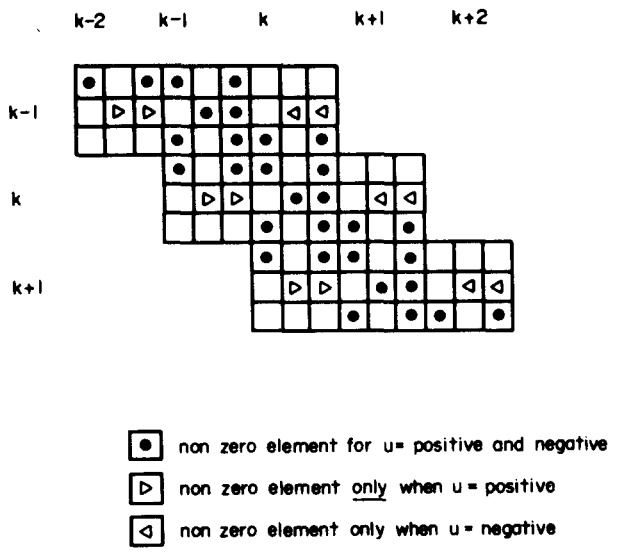

Figure 16. Structure of the diagonal elements.

Comparison with experiments and reference numerical technique

For the first comparison, the predicted and measured pressure histories at the closed end are selected, again from the experiments reported by Edwards & O'Brien (1970). The results of the comparison are shown in figure 5. The characteristic finite difference technique like the explicit finite difference technique, is seen to diffuse the discontinuities predicted by the method of characteristics. However the general features are well predicted. In comparison to the explicit finite difference technique, the characteristic finite difference technique takes much less time for computation. The time steps taken by the characteristic finite difference technique are above the Courant–Fredricks–Lewy limit which averages about 1 ms for this calculation.

The characteristic finite difference scheme has also been compared with the blowdowns performed in the facility shown in figure 6. The pressure histories predicted and observed are shown in figure 7. It is again evident that the characteristic finite differene scheme tends to diffuse the sharp changes predicted by the method of characteristics but the results are otherwise in reasonable agreement. Figure 8 shows the comparisons for mass holdup in the heated section. The method of characteristics and characteristic finite difference calculations are in agreement with each other and the experiment.

It is emphasized again that the differences between the method of characteristics solution and the experimental data are attributed to the mathematical model, i.e. to the idealizations inherent in the homogeneous equilibrium model and the constitutive equations used.

5. MODELLING A COMPLEX REWETTING SITUATION

In this section, we illustrate how mathematical models more complex than those for homoeneous equilibrium flow may be derived from experimental observations.

The physical situation

The process to be modeled occurs when cold water is injected into the hot, horizontal, voided system shown in figure 17. The geometry is of particular interest for Canadian heavy water cooled and moderated reactors, but the methodology followed in deriving the mathematical model is of interest for all systems.

Experiments have been done on cold water injection into such systems with the electrical heaters operating at various power levels and initial temperatures (above rewetting temperatures). All these experiments show the same basis phenomena:

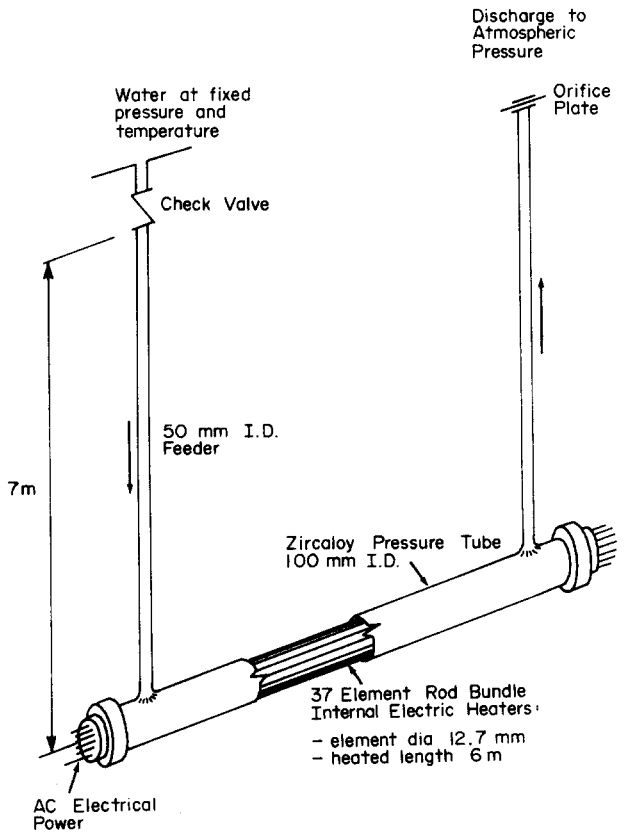

Figure 17. Cold water injection experiment facility.

●the injected water runs along the bottom of the horizontal channel rewetting the lower heated elements and boils once it reaches saturation conditions,

●the steam produced rises towards the top of the horizontal channel and flows along gaining substantial superheat—several hundred degrees above the water temperature,

●both the steam and water streams cool the electrically heated bundle, but the elements in contact with steam see a much lower heat transfer coefficient and are much hotter than those immersed in the water,

●as injection proceeds, the water level rises in the channel and more elements are progressively rewetted starting from the end farthest from the break, till eventually the whole bundle rewets and the channel is filled with water.

These phenomena are illustrated by typical temperature transients measured at various locations in the electrically heated bundle (shown in figure 18).

The field equations

To model the process described, different temperatures must be allowed for each phase in the field equations. Different velocities are not essential because the two streams tend to be homogenized at the heated section exit and entrance by channel hardware such as shield plugs, etc.

The field equations with $u = u_G = u_L$, are

$$\frac{Du}{Dt} + \frac{1}{\rho}\frac{\partial P}{\partial z} = -F - g\frac{dZ}{dz} \equiv C_1, \qquad [31]$$

$$\rho_G \frac{D\alpha}{Dt} + \frac{\alpha}{a_G^2}\frac{DP}{Dt} + \alpha\rho_G \frac{\partial u}{\partial z} = \Gamma_{mG} - \frac{1}{\rho_G}\frac{\partial \rho_G}{\partial h_G}\bigg|_P \{\Gamma_{eG} - (E_G - u^2)\Gamma_{mG} - u\Gamma_{fG}\} - \frac{\alpha\rho_G u}{A}\frac{dA}{dz} \equiv C_4, \qquad [32]$$

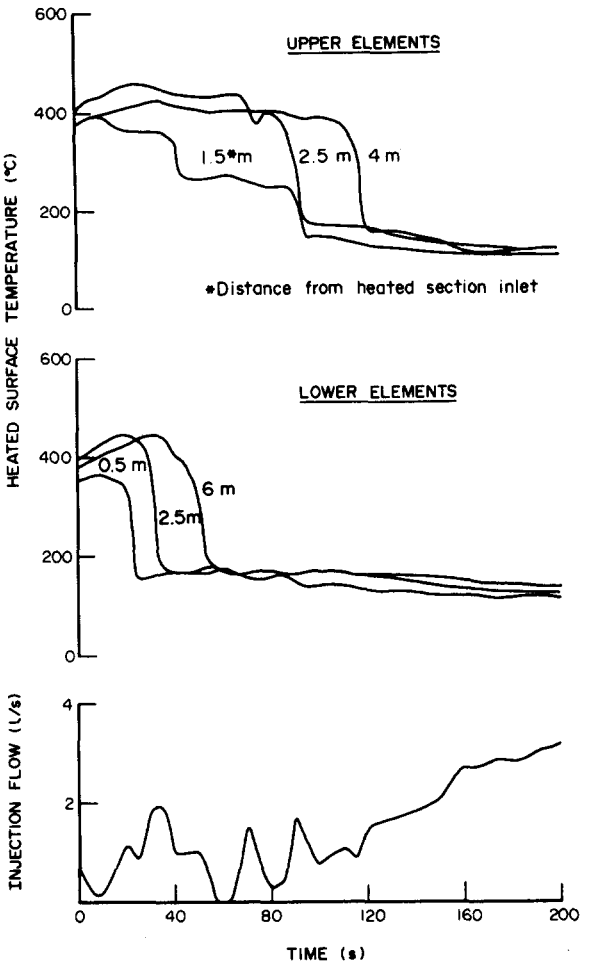

Figure 18. Typical heated surface temperature transients for a horizontal, 37-rod bundle during rewetting.

$$-\rho_L \frac{D\alpha}{Dt} + \frac{1-\alpha}{a_L^2}\frac{DP}{Dt} + (1-\alpha)\rho_L \frac{\partial u}{\partial z} = \Gamma_{mL} - \frac{1}{\rho_L}\frac{\partial \rho_L}{\partial h_L}\bigg|_P \{\Gamma_{eL} - (E_L - u^2)\Gamma_{mL} - u\Gamma_{fL}\}$$

$$-\frac{(1-\alpha)\rho_f u}{A}\frac{dA}{dz} \equiv C_5, \qquad [33]$$

$$\alpha\rho_G \frac{Dh_G}{Dt} - \alpha\frac{DP}{Dt} = \Gamma_{eG} - (E_G - u^2)\Gamma_{mG} - u\Gamma_{fG} \equiv C_6, \qquad [34]$$

$$(1-\alpha)\rho_L \frac{Dh_f}{Dt} - (1-\alpha)\frac{DP}{Dt} = \Gamma_{eG} - (E_f - u^2)\Gamma_{mL} - u\Gamma_{fL} \equiv C_7, \qquad [35]$$

where $E_{L,G} = h_{LG} + u^2/2 + gZ$. The terms of the form Γ_{rk} represent the sum of the rates of transfer of quantity r (m for mass; e for energy; f for momentum) from the wall and interface into phase k per unit volume. They may be written as:

$$\Gamma_{mk} = (m_{wk} + m_{ik}), \qquad [36]$$

$$\Gamma_{ek} = [q_{wk} + q_{ik} + m_{wk}\left(h_k + \frac{u^2}{2} + gZ\right) + m_{ik}\left(h_{ki} + \frac{u^2}{2} + gZ\right) + \tau_{ik}u], \qquad [37]$$

$$\Gamma_{fk} = [-\tau_{wk} - \tau_{ik} + m_{ik}u], \qquad [38]$$

where m and q are the rates of mass and heat transfer per unit volume respectively, and τ is the shear force per unit volume. The subscripts w and i denote transfer from the wall and the

interface respectively. The transfer relationships must conform to

$$\sum_k \Gamma_{mk} = 0; \quad \sum_k \Gamma_{ek} = \sum_k q_{wk}; \quad \sum_k \Gamma_{fk} = -\sum_k \tau_{wk}. \qquad [39]$$

In general the terms Γ_{rk} may be functions of local instantaneous values of the dependent variables and their derivatives. The equations have been phrased with u, P, α, h_G and h_L as the dependent variables so that direct comparison can be made with the compatibility equations [8]–[12] along the characteristics. The equations are more convenient to solve by finite difference techniques when u is replaced by G as a dependent variable.

Constitutive equations

To develop the constitutive equations, appropriate for horizontal channel rewetting, we have used the observed stratification of steam and water phases as shown in figure 19. The temperatures of the steam and water are assumed constant over the cross-section at T_G and T_L respectively. The number of rods in steam is directly related to the void fraction a by:

$$N_G \equiv \alpha N \qquad [40]$$

where N = total number of rods and N_G is an integer. It follows that the number of rods immersed in water is $N_L = N - N_G$.

Heat transfer from rods and at interfaces between steam and water depends on the relationship between:

(i) the rod surface temperature, T_w, and the wetting temperature, T_{wet}, and

(ii) the phase temperatures and the saturation temperature.

For an element j ($j = 1,2,\ldots,N_f$) immersed in water the following possibilities are taken into account:

(i) $T_w > T_{wet}$. The rod is assumed surrounded by a thin steam layer at temperature T_G. The heat transferred from the rod to this layer is

$$(q'_w)_j = p_{rod} h_{wG} (T_{wj} - T_G) \qquad [41]$$

where h_{wG} is an appropriate heat transfer coefficient. At the interface between the steam and

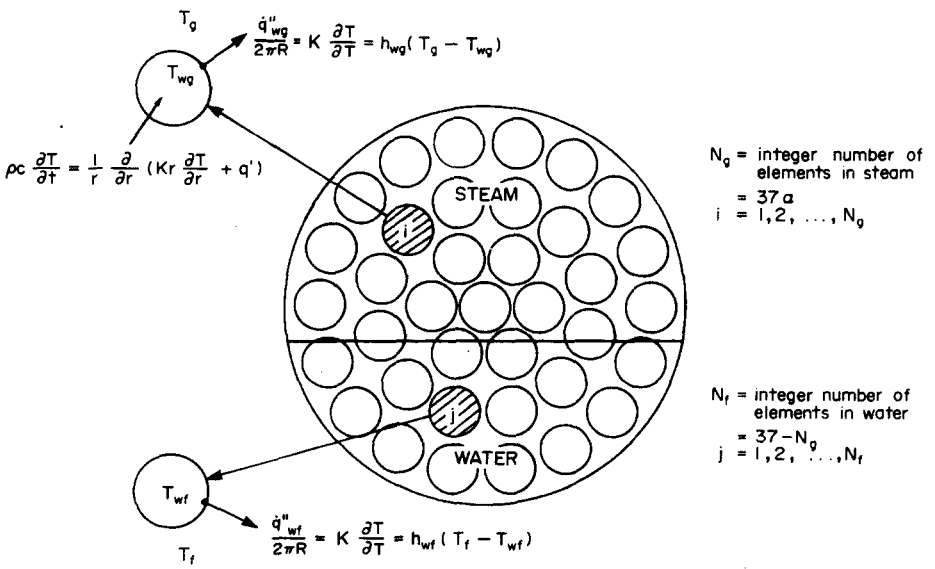

Figure 19. Channel cross-section illustrating modelling for stratified flow.

water (at temperature T_f), the heat transfer is

$$(q'_{iL})_j = p_i h_i (T_s - T_L),$$
$$(q'_{iG})_j = p_i h_i (T_s - T_G) \quad [42]$$

where p_i is the interface perimeter and h_i is an appropriate interfacial heat transfer coefficient. We assume $p_i \sim p_{rod}$. From [42], it follows that the vapour generated at the interface is:

$$(m'_{iG})_j = -(m'_{iL})_j = -\frac{(q'_{iL})_j + (q'_{iG})_j}{h_{LG}} \quad [43]$$

(ii) $T_w < T_{wet}$ and $T_L > T_s$. The surface of the rod is assumed wetted by water at temperature T_L and vapour is generated in the near wall region. The heat transferred from the rod to the water is:

$$(q'_w)_j = p_{rod} h_{wL} (T_{wj} - T_L) \quad [44]$$

The interfacial heat-transfer is again given by [42] using appropriate values for the interfacial perimeter and heat-transfer coefficient. In this case we have again assumed $p_i \sim p_{rod}$. The mass of vapour generated is given by [43].

(iii) $T_w < T_{wet}$ and $T_L < T_s$. The rod is wetted and there is no vapour generated ($p_i = 0$). The heat transferred from the rod to the water is given by [44].

For an element $i (i = 1, 2, \ldots, N_G)$ surrounded by steam at temperature T the heat transferred from the rod is:

$$(q'_w)_i = p_{rod} h_{wG} (T_{wi} - T_G). \quad [45]$$

At any cross-section, the total heat and mass transfer is given by:

$$q_{iL} = \frac{1}{A} \sum_j (q'_{iL})_j \quad [46]$$

$$q_{iG} = \frac{1}{A} \sum_j (q'_{iG})_j, \quad [47]$$

$$q_{wL} = \frac{1}{A} \sum_j (q'_w)_j, \quad [48]$$

$$q_{wG} = \frac{1}{A} \sum_j (q'_w)_i, \quad [49]$$

$$m_{iG} = -m_{iL} = \frac{1}{A} \sum_j (m'_{iG})_j. \quad [50]$$

Both axial and radial heat-conduction within the rods is accounted for by solving the following form of the heat-conduction equation:

$$\rho c \frac{\partial T}{\partial t} = \frac{1}{r} \frac{\partial}{\partial r} \left(K \frac{\partial T}{\partial r} \right) + q' \quad [51]$$

where

$$q' = q_J + K \frac{\partial^2 T}{\partial z^2},$$

q_J = internal heat generated due to Joule effect, K is the thermal conductivity and c is the specific heat. Equation [51] is solved using a finite element procedure. The term $(\partial^2 T/\partial z^2)$ is replaced by a finite difference operator in z which is evaluated at the previous time step.

Solution of the mathematical model and result

We have solved [31]–[35], using the constitutive equations outlined above and an empirical two-phase friction factor, for the horizontal channel shown in figure 17. In this particular application, the flow in the inlet feeder pipes was described by the homogeneous equilibrium model [23]. Both systems of equations were solved using the characteristic finite difference procedure.

Typical upper and lower rod surface temperature transients are shown in figure 20. For the case shown, the system was initially filled with steam at 900 kPa and 275°C. The system was blown down by suddenly opening the outlet to atmosphere. Cold water flow as initiated at the inlet, from a reservoir at 600 kPa and 99°C, when the system pressure reached 600 kPa. As may be seen from figure 20 the predicted temperature transients have the same features as those observed experimentally. We conclude from these results that the mathematical model adequately represents the physical system. We are continuing our work to refine the rod-to-flow and interphase heat-transfer coefficients.

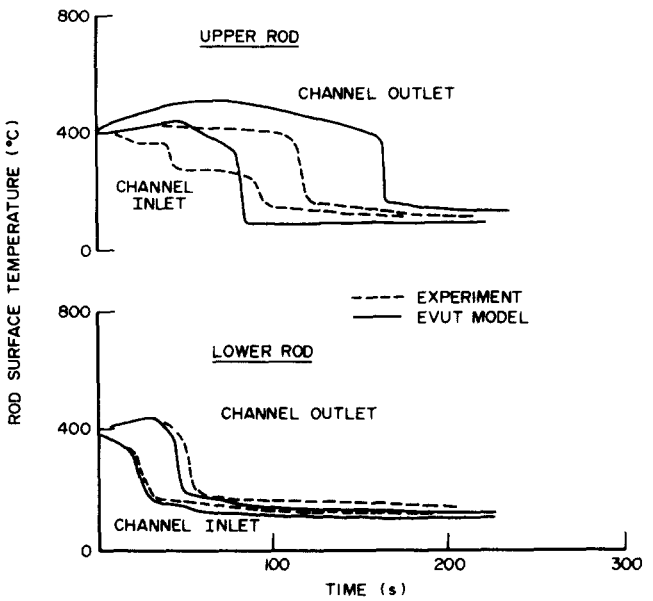

Figure 20. Typical predictions for heated surface temperature transients.

6. SUMMARY

Methods for analysing transient two-phase flow, developed in Canada, have been discussed in this paper. A reference numerical technique (the method of characteristics) has been described and its role in developing mathematical models and more practical numerial techniques has been discussed. Computationally faster and adequately accurate numerical techniques called "explicit finite difference" and an implicit form called "characteristic finite difference" have been described. One dimensional field equations with equal phase velocities appear to be adequate in predicting the experiments with which comparisons have been made. Development of simple constitutive equations based on flow regime and a physical understanding of the phenomena occuring in a complex situation has been discussed.

Our main conclusions are:

●for calculations of flows with high velocities such as during the earlier stages of

blowdown, one dimensional mathematical models with equal phase velocities appear to be adequate;

● for such flows, thermal non-equilibrium between phases may have to be considered for some special applications, but the homogeneous equilibrium model predicts the main trends well;

● when thermal non-equilibrium is considered, the constitutive equations should be based on flow regimes and the physical processes observed in experiments;

● for lower velocity flows, unequal phase velocities may have to be considered.

The last conclusion indicates the direction for future Canadian work.

NOMENCLATURE

A cross section area (m^2);

a homogeneous equilibrium sound speed $\equiv \left[\frac{1}{\rho}\frac{\partial \rho}{\partial H}\Big|_P + \frac{\partial \rho}{\partial P}\Big|_H\right]^{-1/2}$ (m/s);

a' homogeneous non-equilibrium sound speed $\equiv \left[\rho\left(\frac{1-\alpha}{\rho_L a_L^2} + \frac{\alpha}{\rho_G a_G^2}\right)\right]^{-1/2}$ (m/s);

a_k phase k sound speed $\equiv \left[\frac{1}{\rho_k}\frac{\partial \rho_k}{\partial h_k}\Big|_P + \frac{\partial \rho_k}{\partial P}\Big|_{h_k}\right]^{-1/2}$ (m/s);

c specific heat (J/kg.K);

d_e equivalent diameter (m);

e mixture internal energy $\equiv$ x $e_G + (1-x)e_L$(J/kg);

E $\equiv \rho\left(e + \frac{(Gv')^2}{2}\right)$;

F friction force per unit mass (m/s^2);

f friction factor;

g acceleration of gravity (m/s^2);

G mass velocity (kg/m^{2}s);

h heat-transfer coefficient (W/m^{2}K);

h_k phase k enthalpy (J/kg);

h_{LG} latent heat of vaporization (J/kg);

H mixture enthalpy $\equiv X\, h_g + (1-X)\, h_g$;

K thermal conductivity (w/m^{2}K)

m mass generation rate per unit volume (kg/m^{3}s);

P perimeter (m);

N number of rods;

P pressure (Pa);

Q heat added per unit mass (W/kg);

q heat added per unit volume (W/m^3);

r radial coordinate (m);

R rod radius (m);

t time (s);

T temperature (°C);

u velocity (m/s);

v mixture specific volume $\equiv xv_G + (1-x)v_L$ (m^3/kg);

v_k phase k specific volume (m^3/kg);

x thermodynamic quality;

X flow quality;

z space coordinate (m);

Z elevation (m);

α void fraction;

ρ mixture density $\equiv \alpha\rho_G + (1-\alpha)\,\rho_L$ (kg/m^3);

ρ_k phase k density (kg/m^3);

τ frictional force per unit volume (N/m^3);

μ viscosity (kg/ms).

Subscripts

L liquid phase;

G vapour phase;

s saturation condition;

w wall;

i interface.

REFERENCES

AEROJET NUCLEAR COMPANY 1974 March 1974 Water Reactor Safety Research Report, Idaho Falls, Idaho.

ARRISON, N. L., HANCOX, W. T., SULATISKY, M. T. & BANERJEE, S. 1977 Blowdown of a recirculating

loop with heat addition. Paper 61 Thermodynamics and Fluid Mechanics Group Conference, University of Manchester.

BANERJEE, S., HANCOX, W. T., JEFFRIES, R. B., & SULATISKY, M. T. 1975 Transient two-phase flow and heat transfer during blowdown from subcooled conditions with heat addition A.I.Ch.E. paper 24, 15th National Heat Transfer Conference, San Francisco.

BOURE, J. A. 1975 On a unified presentation of the non-equilibrium two-phase flow models. Proceedings of the A.S.M.E. Symposium on Non-Equilibrium Two-Phase Flows, Houston, 1–9.

BRITTIAN, I., & FAYERS, F. J. 1976 A review of U.K. developments in thermal-hydraulic methods for loss of coolant accidents. Proceedings of the CSNI Specialists Meeting on Transient Two-Phase Flow, Toronto. Atomic Energy of Canada Ltd., Toronto.

EDWARDS, A. R., & O'BRIEN, T. P. 1970 Studies of Phenomena Connected with the Depressurization of Water Reactors. *J. B. Nucl. Energy Soc.* **9**, 125–135.

ELLIOTT, J. N. 1968 RODFLOW. A program for studying transients in a power reactor coolant circuit. Unpublished AECL internal report, Sheridan Park.

FERCH, R. L. 1978 Method of characteristics solutions for non-equilibrium transient flow-boiling, submitted for publication.

HANCOX, W. T., MATHERS, W. G., & KAWA, D. 1975 Analysis of transient flow-boiling; application of the method of characteristics, A.I.Ch.E. paper 42, 15th National Heat Transfer Conference, San Francisco.

MATHERS, W. G., ZUZAK, W. W., MCDONALD, B. H. & HANCOX, W. T. 1976 On finite difference solutions to the transient flow-boiling equations, proceedings of the CSNI Specialists Meeting on Transient Two-Phase Flow, Toronto. Atomic Energy of Canada Ltd., Toronto.

MOORE, K. V., & RETTIG, W. H. 1973 A computer program for transient thermal-hydraulic analysis, Aerojet Nuclear Company Report, ANCR-1127.

PREMOLI, A., & HANCOX, W. T. 1976 An experiment investigation of subcooled blowdown with heat addition, proceedings of the CSNI specialists meeting on transient two-phase flow, Toronto. Atomic Energy of Canada Ltd., Toronto.